Direct Observation of Ultrafast Decarboxylation of Acyloxy Radicals *via* Photoinduced Electron Transfer in Carboxylate Ion Pairs

T. Michael Bockman, Stephan M. Hubig, and Jay K. Kochi*

Department of Chemistry, University of Houston, Houston, Texas 77204-5641

Received September 17, 1996[⊗]

Charge-transfer (CT) photoactivation of the electron donor−acceptor salts of methylviologen (MV^{2+}) with carboxylate donors (RCO_2^-) including benzilates [$Ar_2C(OH)CO_2^-$] and arylacetates ($ArCH_2CO_2^-$) leads to transient [$MV^{\bullet+}$, $RCO_2^{\bullet}$] radical pairs. Femtosecond time-resolved spectroscopy reveals that the photogenerated acyloxy radicals ($RCO_2^{\bullet}$) rapidly lose carbon dioxide by C−CO_2 bond cleavage, in competition with back-electron transfer to restore the original ion pair, [MV^{2+}, RCO_2^-]. The decarboxylation rate constants for $ArCH_2CO_2^{\bullet}$ lie in the range $(1-2) \times 10^9$ s^{-1}, in agreement with previous reports. In striking contrast, the C−CO_2 bond scission in $Ar_2C(OH)CO_2^{\bullet}$ occurs within a few picoseconds ($k_{CC} = (2-8) \times 10^{11}$ s^{-1}). The rate constants for decarboxylation of these donors approach those of barrier-free unimolecular reactions. Thus, real-time monitoring of the decarboxylation of benziloxy radicals represents the means for the direct observation of the transition state for C−C bond scission.

Introduction

Recent advances in laser spectroscopy on the picosecond and femtosecond time scales[1,2] have made it possible to monitor in real time the course of a single reaction step, from reactants to products through the transition state.[3] Electron transfer,[4] bond scission,[5] proton transfer,[6] and structural isomerization[7] are among the elementary reactions that have been successfully analyzed by the use of the new time-resolved techniques. A process of fundamental importance that can be observed by this experimental approach is carbon−carbon bond cleavage, and the loss of carbon dioxide from acyloxy radicals, i.e.,

$$RCO_2^{\bullet} \xrightarrow{k_{CC}} R^{\bullet} + CO_2 \qquad (1)$$

is an example that has recently drawn considerable interest.[8−11] Previous indirect measurements have shown that this decarboxylation process takes place on time scales of less than 1 ns.[8−11] In order to monitor directly the rapid fragmentation in eq 1, a means of generating the reactive radical, $RCO_2^{\bullet}$, on very short time scales—picoseconds to femtoseconds—is thus required. This goal is accomplished by one-electron oxidation of the corresponding carboxylate anion (RCO_2^-), which is instantaneously[12] effected by the charge-transfer photoactivation ($h\nu_{CT}$) of its preformed complex with an electron acceptor (A).[13−16] Excitation of such electron donor−acceptor (EDA) complexes can thus be employed to convert a carboxylate anion to the corresponding acyloxy radical, i.e.,

[⊗] Abstract published in *Advance ACS Abstracts,* March 15, 1997.

(1) Manz, J.; Wöste, L. *Femtosecond Chemistry*; VCH: Weinheim, 1995.

(2) Simon, J. D. *Rev. Sci. Instrum.* **1989**, *60*, 3597.

(3) (a) Zewail, A. H. *J. Phys. Chem.* **1993**, *97*, 12427. (b) Kaiser, W. *Ultrashort Laser Pulses and Applications*; Springer: New York, 1988. (c) Martin, J.-L.; Migus, A.; Mourou, G. A.; Zewail, A. H. *Ultrafast Phenomena VIII*; Springer: New York, 1993.

(4) (a) Kliner, D. A. V.; Alfano, J. C.; Barbara, P. F. *J. Chem. Phys.* **1993**, *98*, 5375. (b) Schoenlein, R. W.; Peteanu, L. A.; Wang, Q.; Mathies, R. A.; Shank, C. V. *J. Phys. Chem.* **1993**, *97*, 12087. (c) Joly, A. G.; Nelson, K. A. *Chem. Phys.* **1991**, *152*, 69. (d) Zhang, H.; Jonkman, A. M.; van der Meulen, P.; Glasbeek, M. *Chem. Phys. Lett.* **1994**, *224*, 551. (e) Reid, P. J.; Barbara, P. F. *J. Phys. Chem.* **1995**, *99*, 3554. (f) Walker, G. C.; Barbara, P. F.; Doorn, S. K.; Dong, Y.; Hupp, J. T. *J. Phys. Chem.* **1991**, *95*, 5712. (g) Wynne, K.; Galli, C.; Hochstrasser, R. M. *J. Chem. Phys.* **1994**, *100*, 4797. (h) Sakata, Y.; Tsue, H.; Oneil, M. P.; Wiederrecht, G. P.; Wasielewski, M. R. *J. Am. Chem. Soc.* **1994**, *116*, 6904. (i) Laermer, F.; Elsaesser, T.; Kaiser, W. *Chem. Phys. Lett.* **1988**, *148*, 119

(5) (a) Pederson, S.; Baumert, T.; Zewail, A. H. *J. Chem. Phys.* **1993**, *97*, 12460. (b) Dantus, M.; Rosker, M. J.; Zewail, A. H. *J. Chem. Phys.* **1988**, *89*, 6128. (c) Banin, U.; Ruhman, S. *J. Chem. Phys.* **1993**, *98*, 4391. (d) King, J. C.; Zhang, J. Z.; Schwartz, B. J.; Harris, C. B. *J. Chem. Phys.* **1993**, *99*, 7595. (e) Dougherty, T. P.; Heilweil, E. J. *Chem. Phys. Lett.* **1994**, *227*, 19. (f) Lenderink, E.; Duppen, K.; Wiersma, D. A. *Chem. Phys. Lett.* **1993**, *211*, 503

(6) Schwartz, B. J.; Peteanu, L. A.; Harris, C. B. *J. Phys. Chem.* **1992**, *96*, 3591.

(7) Sension, R. J.; Repinec, S. T.; Szarka, A. Z.; Hochstrasser, R. M. *J. Chem. Phys.* **1993**, *98*, 6291.

(8) (a) Braun, W.; Rajbenbach, L.; Eirich, F. R. *J. Phys. Chem.* **1962**, *66*, 1591. (b) Kaptein, R.; Brokken-Zijp, J.; de Kanter, F. J. J. *J. Am. Chem. Soc.* **1972**, *94*, 6280. See also: (c) Sheldon, R. A.; Kochi, J. K. *J. Am. Chem. Soc.* **1970**, *92*, 5175.

(9) Falvey, D. E.; Schuster, G. B. *J. Am. Chem. Soc.* **1986**, *108*, 7419.

(10) Hilborn, J. W.; Pincock, J. A. *J. Am. Chem. Soc.* **1991**, *113*, 2683.

(11) (a) Chateauneuf, J.; Lusztyk, J.; Ingold, K. U. *J. Am. Chem. Soc.* **1987**, *109*, 897. (b) Chateauneuf, J.; Lusztyk, J.; Ingold, K. U. *J. Am. Chem. Soc.* **1988**, *110*, 2886. (c) Tateno, T.; Sakuragi, H.; Tokumaru, K. *Chem. Lett.* **1992**, 1883. (d) Rauk, A.; Yu, D.; Armstrong, D. A. *J. Am. Chem. Soc.* **1994**, *116*, 8222. (e) Davidson, R. S.; Steiner, P. R. *J. Chem. Soc., Perkin Trans. 2* **1971**, 1357. (f) Prasad, D. R.; Hoffman, M. Z.; Mulazzani, Q. G.; Rodgers, M. A. J. *J. Am. Chem. Soc.* **1986**, *108*, 5135. For a comprehensive review of photodecarboxylations, see: (g) Budac, D.; Wan, P. *J. Photochem. Photobiol. A* **1992**, *67*, 135.

(12) Time-resolved spectroscopy[4g,15] has established that CT excitation of the EDA complex effects the transfer of an electron from the donor to the acceptor in less than 500 fs.

(13) Mulliken theory describes the linear relationship between the charge-transfer transition energies ($h\nu_{CT}$) of these new absorption bands and the electron-richness of the donors, as measured by their ionization potentials (IP) in the gas phase and their thermodynamic oxidation potentials ($E°_{ox}$) in solution. See: (a) Mulliken, R. S. *J. Am. Chem. Soc.* **1952**, *74*, 811. (b) Mulliken, R. S.; Person, W. B. *Molecular Complexes: A Lecture and Reprint Volume*; Wiley: New York, 1969.

(14) (a) Hilinski, E. F.; Masnovi, J. M.; Amatore, C.; Kochi, J. K.; Rentzepis, P. M. *J. Am. Chem. Soc.* **1983**, *105*, 6167. (b) Hilinski, E. F.; Masnovi, J. M.; Kochi, J. K.; Rentzepis, P. M. *J. Am. Chem. Soc.* **1984**, *106*, 8071. (c) Hubig, S. M.; Bockman, T. M.; Kochi, J. K. *J. Am. Chem. Soc.* **1996**, *118*, 3842.

(15) (a) Ojima, S.; Miyasaka, H.; Mataga, N. *J. Phys. Chem.* **1990**, *94*, 4147. (b) Ojima, S.; Miyasaka, H.; Mataga, N. *J. Phys. Chem.* **1990**, *94*, 5834. (c) Ojima, S.; Miyasaka, H.; Mataga, N. *J. Phys. Chem.* **1990**, *94*, 7534.

(16) Ebbesen, T. W.; Manring, L. E.; Peters, K. S. *J. Am. Chem. Soc.* **1984**, *106*, 7400.

S0022-3263(96)01783-5 CCC: $14.00 © 1997 American Chemical Society

$$[RCO_2^-, A] \xrightarrow{h\nu_{CT}} [RCO_2^\bullet, A^{-\bullet}] \quad (2)$$

This novel method for the photogeneration of the acyloxy radical (eq 2) contrasts with other photochemical methods, such as the cleavage of peroxides,[9] esters,[10] etc., since it yields the reactive radicals in their electronic ground states.[17]

Earlier reports noted the formation of EDA complexes[18−20] between carboxylate donors and the dicationic acceptor, 1,1′-dimethyl-4,4′-bipyridinium, commonly referred to as methylviologen (MV^{2+}).[21−23] [Such EDA complexes between negatively-charged donors and positively-charged acceptors constitute charge-transfer (CT) ion pairs.] The properties of the CT ion pair formed between MV^{2+} and the benzilate anion ($Ph_2C(OH)CO_2^-$) were particularly intriguing, since its photolysis led to the efficient ($\phi = 0.8-1.2$) formation of decarboxylation products.[18] Moreover, the characteristic absorption spectrum of reduced methylviologen ($A^{\bullet-} = MV^{\bullet+}$ in eq 2)[22] provides a means of monitoring the reaction by time-resolved pump-probe absorption spectroscopy. To access the critical femtosecond/picosecond time scales relevant to electron transfer and bond cleavage, we designed and constructed a time-resolved femtosecond spectrometer based on a Ti:sapphire laser with a short (230 fs) pulse and a broad tuning range (360−450 nm, frequency-doubled) as the excitation source. We chose a laser system with a high-energy pulse, which allowed us to record a continuous visible spectrum (360−900 nm) in a single laser shot. This approach not only provided kinetic traces at all relevant wavelengths, but more importantly, it enabled us to recognize subtle spectral changes in the intermediates during the decarboxylation process.[23]

Results

To prepare the methylviologen benzilate ion pairs, a series of benzilic acids, $Ar_2C(OH)CO_2H$, with electron-donating substituents on the aromatic rings were synthesized. The carboxylate anions were generated *in situ* by dissolution of the free carboxylic acids in aqueous sodium bicarbonate. Methylviologen was prepared and used as the bis(trifluoromethanesulfonate) or ditriflate salt, $MV(OTf)_2$.[24] The benzilate substrates are shown in Chart 1.

Chart 1

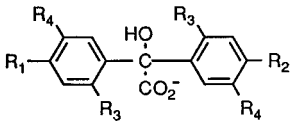

Benzilate:
$R_1=R_2=R_3=R_4=H$

4,4'-Dimethylbenzilate:
$R_1=R_2=Me$; $R_3=R_4=H$

4-Methoxybenzilate:
$R_1=R_3=R_4=H$; $R_2=OMe$

4,4'-Dimethoxybenzilate
$R_1=R_2=OMe$; $R_3=R_4=H$

2,2',5,5'-Tetramethoxybenzilate:
$R_1=R_2=H$; $R_3=R_4=OMe$

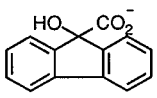

9-Hydroxyfluorene-carboxylate

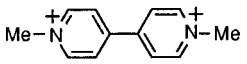

Methylviologen (MV^{2+})

I. Charge-Transfer Bands of Methylviologen/Carboxylate Ion Pairs. When the colorless methylviologen ditriflate was added to an aqueous solution of sodium benzilate, a light yellow color developed immediately. ^{1}H-NMR analysis of the colored solution (in D_2O) showed no changes in the proton resonances of MV^{2+} or of the benzilate anion [compared with those of pure $MV(OTf)_2$ or $Ph_2C(OH)CO_2Na$]. The intensity of the yellow color faded upon extensive dilution or upon the addition of inert salt. By analogy with previous observations,[25] the color change was attributed to the formation of an ion pair[26,27] between the positively charged methylviologen and the negatively charged benzilate, *i.e.*

$$MV^{2+} + Ar_2C(OH)CO_2^- \overset{K_{IP}}{\rightleftharpoons} [MV^{2+}, Ar_2C(OH)CO_2^-] \quad (3)$$

UV−vis spectroscopy revealed that the yellow color was caused by a new electronic absorption band in the spectral region between 340 and 420 nm, where neither $MV(OTf)_2$ nor $Ph_2C(OH)CO_2Na$ absorbed. Similar color changes were observed upon addition of methylviologen to other substituted benzilate anions in aqueous solution. Figure 1 shows the visible absorption bands of the ion pairs in eq 3, with their progressive red shift as the anion is changed from benzilate (Ar = phenyl) to 4,4′-dimethoxybenzilate (Ar = *p*-anisyl) and to 2,2′,5,5′-tetramethoxybenzilate (Ar = 2,5-dimethoxyphenyl). Such a red shift as the aromatic nucleus becomes progressively more electron-rich accords with the Mulliken theory[13] of charge-transfer interactions. This charge-transfer theory further implies that irradiation of the new absorption bands in Figure 1 effects the transfer of a single electron from the benzilate donor to the viologen acceptor, according to the Mulliken formulation in eq 4.

$$[MV^{2+}, Ar_2C(OH)CO_2^-] \xrightarrow{h\nu_{CT}} [MV^{+\bullet}, Ar_2C(OH)CO_2^\bullet] \quad (4)$$

Therefore, the methylviologen/benzilate ion pairs were identified as *charge-transfer* (CT) ion pairs.[27]

(17) Bond homolysis by the direct photoexcitation of these precursors involves excited states, the temporal relaxation of which leads to the acyloxy radical on the same time scale as the cleavage process itself. The overall kinetics of the photodecarboxylation is thus a convolution of the formation as well as the decomposition of the acyloxy radical, and rate constants (k_{CC}) on the picosecond time scale cannot be readily extracted. For a discussion of this problem in the context of peroxide decomposition, see ref 9.

(18) Barnett, J. R.; Hopkins, A. S.; Ledwith, A. *J. Chem. Soc., Perkin Trans. 2* **1973**, 80.

(19) (a) Deronzier, A.; Esposito, F. *Nouv. J. Chem.* **1983**, *7*, 15. (b) Jones, G., II; Zisk, M. B. *J. Org. Chem.* **1986**, *51*, 947. (c) Mandler, D.; Willner, I. *J. Chem. Soc., Perkin Trans. 2* **1988**, 997. (d) Ford, W. E.; Rodgers, M. A. J. *J. Phys. Chem.* **1991**, *95*, 5827.

(20) Usui, Y.; Sasaki, Y.; Ishii, Y. Tokumaru, K. *Bull. Chem. Soc. Jpn.* **1988**, *61*, 3335.

(21) (a) Michaelis, L. *Biochem. Z.* **1932**, *250*, 564. (b) Michaelis, L.; Hill, E. S. *J. Gen. Physiol.* **1933**, *16*, 859.

(22) (a) Watanabe, T.; Honda, K. *J. Phys. Chem.* **1982**, *86*, 2617. (b) Bockman, T. M.; Kochi, J. K. *J. Org. Chem.* **1990**, *55*, 4127.

(23) See Bockman, T. M.; Hubig, S. M.; Kochi, J. K. *J. Am. Chem.Soc.* **1996**, *118*, 4502 for a preliminary report of these results.

(24) In contrast to the more commonly-utilized chloride or bromide salts,[24b] methylviologen triflate showed no interfering CT bands between anion and cation. (b) Ebbesen, T. W.; Ferraudi G. *J. Phys. Chem.* **1983**, *87*, 3717.

(25) (a) Bockman, T. M.; Kochi, J. K. *J. Am. Chem. Soc.* **1989**, *111*, 4669. (b) Kochi, J. K.; Bockman, T. M. *Adv. Organomet. Chem.* **1991**, *33*, 51.

(26) Kosower, E. M. *J. Am. Chem. Soc.* **1956**, *80*, 3253.

(27) The possibility of further aggregation (to form triple ions, ion quadrupoles, etc.) is unlikely in view of the high polarity of the aqueous medium and the relatively low concentrations (<0.1 M) of methylviologen and benzilate salts needed to observe the CT absorption bands. [Triple-ion formation constants for MV^{2+} and halide anions are on the order of 1.0 M^{-1}. See ref 24b.]

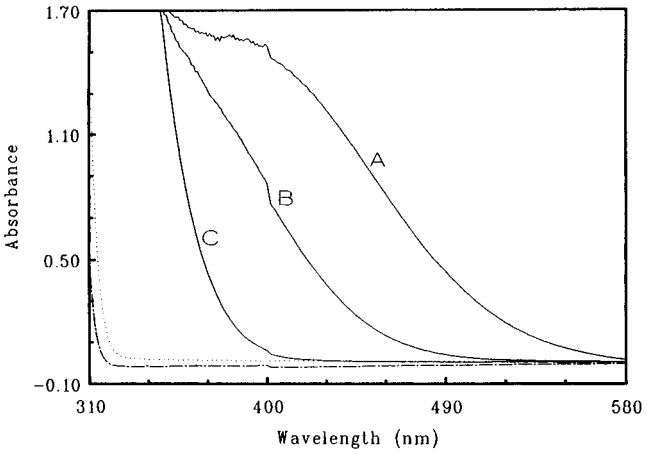

Figure 1. Charge-transfer absorption spectra of methylviologen (0.05 M) in aqueous solution ion-paired with (A) 2,2′,5,5′-tetramethoxybenzilate, (B) 4,4′-dimethoxybenzilate, and (C) benzilate. The dashed lines are the spectral cutoffs of methylviologen ditriflate (···) and sodium tetramethoxybenzilate (−·−).

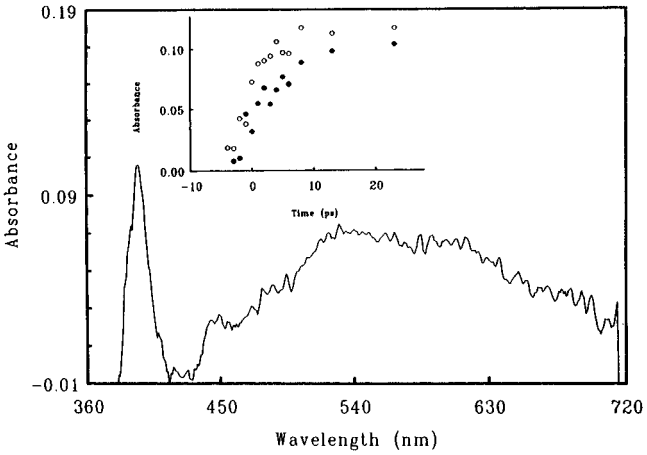

Figure 2. Transient absorption spectrum recorded 1.0 ps following the 230-fs laser excitation (375 nm) of MV^{2+}/benzilate CT ion pairs in aqueous solution. The inset shows the rise (**P**-behavior) of the absorption of $MV^{\bullet+}$, monitored at 605 nm (open circles), and the rise of benzophenone ketyl radical, monitored at 530 nm (closed circles).

Charge-transfer ion pairs were also formed upon addition of $MV(OTf)_2$ to aqueous solutions of sodium arylacetates ($ArCH_2CO_2Na$). An increasing red shift in the CT absorption band was observed as the *para* substituent was changed in the order Cl < H < Ph < OMe. The CT absorption bands of the [MV^{2+}, benzilate] ion pairs could not be distinguished from those of the arylacetates with the same ring substituents. Thus, the CT bands of methylviologen benzilate and phenylacetate were both observed as broad tailing bands, extending from 340 to 420 nm, while the bands of the ion pairs formed from 4,4′-dimethoxybenzilate and 4-methoxyphenylacetate both had distinct maxima at $\lambda_{max} = 370$ nm.

II. Femtosecond Transient Spectroscopy and Kinetics of [MV^{2+}, $Ar_2C(OH)CO_2^-$] Ion Pairs. Benzilate and 4,4′-Dimethylbenzilate. Immediately upon 375-nm laser photolysis of the CT ion pair formed from methylviologen and benzilate ions, the transient spectrum shown in Figure 2 was observed. The spectrum exhibited two bands: a strong, sharp band with $\lambda_{max} =$ 390 nm and a broad absorbance in the visible region,

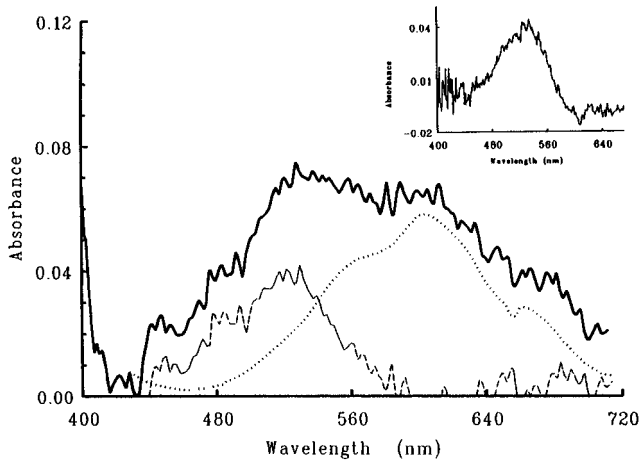

Figure 3. Deconvolution of the 600-nm band in Figure 2 as the sum of the absorbance of methylviologen (dotted spectrum) and benzophenone ketyl radical (dashed spectrum). The inset shows the authentic spectrum of the ketyl radical observed 55 ps following charge-transfer irradiation (355 nm) of the [N-methyl-4-cyanopyridinium, benzilate] ion pair.

centered at $\lambda \approx 600$ nm. The first band was readily identified as the near-UV absorption band of the reduced form of methylviologen ($MV^{\bullet+}$), the absorption spectrum of which has two maxima (390 and 605 nm)[22] in aqueous solution. Subtraction of the visible absorbance of $MV^{\bullet+}$ from the composite 600 nm band (see Figure 3) yielded an additional absorption band ($\lambda_{max} = 530$ nm), which was identified as the visible band of the ketyl radical $Ph_2C(OH)^{\bullet}$ (*vide infra*). Since the formation of the ketyl radical and $MV^{\bullet+}$ were both observed on the early picosecond time scale, we conclude that the transfer of an electron from the benzilate anion to methylviologen was accompanied by decarboxylation, i.e.,

$$[MV^{2+}, Ph_2C(OH)CO_2^-] \xrightarrow{h\nu_{CT}} [MV^{+\bullet}, Ph_2C(OH)^{\bullet}, CO_2] \quad (5)$$

The derived extinction coefficient of $\epsilon_{530} = 6200\ M^{-1}\ cm^{-1}$ for the ketyl radical in Figure 3 was in reasonable agreement with the reported value of $5500\ M^{-1}\ cm^{-1}$,[28] and, thus, confirmed the equimolar formation of $MV^{\bullet+}$ and $Ph_2C(OH)^{\bullet}$ in eq 5. The formation of $MV^{\bullet+}$ and $Ph_2C(OH)^{\bullet}$ could be separately monitored by following the absorbance changes at 605 and 530 nm, respectively. The inset to Figure 2 shows that the rise of the $MV^{\bullet+}$ absorbance occurred on the same time scale (700 fs) as the instrumental response of the laser system, but the growth of the ketyl radical absorbance was significantly retarded. The absorbance of both species reached a maximum after 3 ps and remained unchanged throughout the observation time window of 50 ps.[29]

Nearly identical transient spectra and kinetics were obtained upon CT-photolysis of the ion pair formed from MV^{2+} and 4,4′-dimethylbenzilate. In this case, the absorption band of the ketyl radical ($\lambda_{max} = 550$ nm) and that of $MV^{\bullet+}$ ($\lambda_{max} = 605$ nm) grew in with the same risetime as the response time of the laser spectrometer

(28) Hayon, E.; Ibata, T.; Lichtin, N. N.; Simic, M. *J. Phys. Chem.* **1972**, *76*, 2072.

(29) (a) Since the experimental spectrum in Figure 2 was unchanged over a period of more than 50 ps, a correction for group velocity dispersion[29b] was unnecessary. (b) Sharma, D. K.; Yip, R. W.; Williams, D. F.; Sugamori, S. E.; Bradley, L. L. T. *Chem. Phys. Lett.* **1976**, *41*, 460

(700 fs). Both transient bands persisted unchanged in intensity and appearance for times exceeding 50 ps.

The spectrum of the ketyl radical derived from benzilate could be more clearly distinguished in the absence of strongly-absorbing $MV^{\bullet+}$. Thus, 355-nm excitation[30] of the charge-transfer band of benzilate paired with the (monocationic) acceptor *N*-methyl-4-cyanopyridinium (NCP^+) generated a transient band ($\lambda_{max} = 530$ nm; see inset to Figure 3) identical to the (deconvoluted) band of $Ph_2C(OH)^\bullet$ generated from the corresponding [MV^{2+}, benzilate] ion pair in Figure 3. The ketyl radical was generated by CT excitation, in the same manner as described for the MV^{2+} ion pairs, i.e.,

$$[NCP^+, Ph_2C(OH)CO_2^-] \xrightarrow{h\nu_{CT}} [NCP^\bullet, Ph_2C(OH)^\bullet, CO_2] \quad (6)$$

In this experiment, however, only the absorption band of the ketyl radical was observed, since the $NCP^\bullet$ radical does not absorb visible light.[31] To confirm the assignment of the 530- and 550-nm transients to the ketyl radicals, diphenylhydroxymethyl and bis(4-methylphenyl)hydroxymethyl were generated independently by photolysis of benzophenone and 4,4′-dimethylbenzophenone,[32,33] respectively, in aqueous isopropyl alcohol. (See the Experimental Section.) The absorption spectra of these transients were identical to the ketyl spectra generated from the MV^{2+} and NCP^+ ion pairs.

In summary, the spectroscopic and kinetic behavior of MV^{2+} ion pairs with both benzilate and 4,4′-dimethylbenzilate followed a pattern characterized by (1) simultaneous or near-simultaneous formation of $MV^{\bullet+}$ and $Ar_2C(OH)^\bullet$ on a time scale comparable to the risetime of the laser pulse followed by (2) persistence of both species for long times ($t > 50$ ps). This behavior is labeled **P** to denote the persistence of the transients.

2,2′,5,5′-Tetramethoxybenzilate and 9-Hydroxy-9-fluorenecarboxylate. Quite different behavior was observed upon excitation of the CT ion pair formed from MV^{2+} and 2,2′,5,5′-tetramethoxybenzilate. Photostimulation at $\lambda = 398$ nm led to the formation of $MV^{\bullet+}$, but the ketyl radical was not observed. (See Figure 4.) The undistorted transient spectrum of $MV^{\bullet+}$ decayed to the spectral base line within 5 ps after laser excitation. This decay was fitted to a first-order rate law, and the lifetime of $MV^{\bullet+}$ was calculated as $\tau_{MV} = 1.9$ ps. Analogous results were obtained upon photolysis of the charge-transfer band of MV^{2+} with 9-hydroxy-9-fluorenecarboxylate. The undistorted spectrum of $MV^{\bullet+}$ decayed to the base line by simple first-order kinetics ($\tau_{MV} = 20$ ps), and the fluorenone ketyl radical was not present.[34] This pattern of behavior, characterized by the formation of $MV^{\bullet+}$ unaccompanied by ketyl radical, and the subsequent decay of its absorbance, is labeled **D** to emphasize the complete disappearance of the spectral transient.

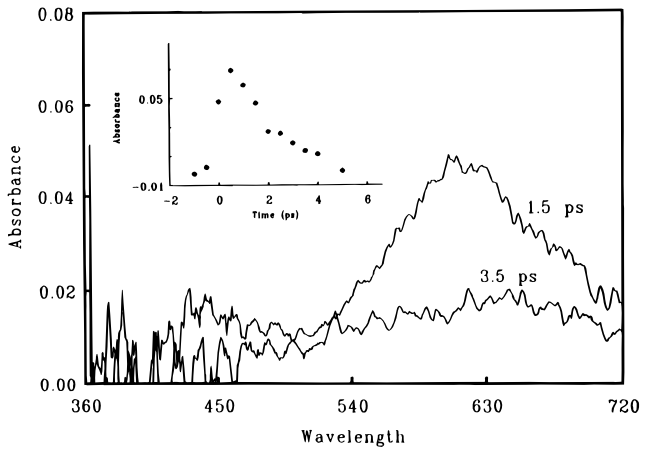

Figure 4. Transient absorption spectra recorded following the 230-fs laser excitation (398 nm) of MV^{2+}/2,2′,5,5′-tetramethoxybenzilate CT ion pairs in aqueous solution. [The narrow UV absorption band of $MV^{\bullet+}$ at 395 nm is obscured by scattered light from the laser excitation pulse.] The inset shows the rise and decay (**D**-behavior) of the absorbance of $MV^{\bullet+}$ monitored at 605 nm.

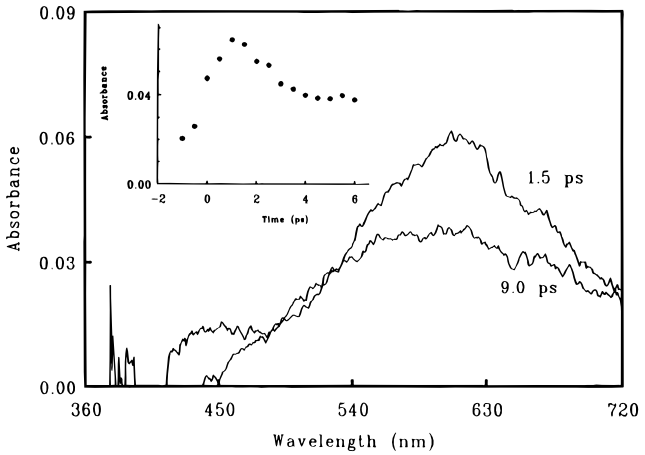

Figure 5. Transient absorption spectra recorded following the 230-fs laser excitation (398 nm) of MV^{2+}/4,4′-dimethoxybenzilate CT ion pairs in aqueous solution. (The narrow UV absorption band of $MV^{\bullet+}$ at 395 nm is obscured by scattered light from the laser excitation pulse.) The inset shows the rise and partial decay (**DP**-behavior) of the absorbance of $MV^{\bullet+}$ monitored at 605 nm.

4,4′-Dimethoxybenzilate and 4-Methoxybenzilate. A third type of behavior characterized these CT ion pairs. At early times ($t < 5$ ps), $MV^{\bullet+}$ was the only transient observed, and its spectrum decayed to a residual absorbance within 5 ps. During this decay process, the spectral band of $MV^{\bullet+}$ centered at 600 nm underwent a distinct broadening, as shown in Figure 5. No further evolution of the transient absorption was observed, and the broad band persisted unchanged for times greater than 50 ps after the laser pulse. The broadening of the band at longer time intervals was attributed to the absorption of the ketyl radicals, $Ar_2C(OH)^\bullet$ (Ar = anisyl

(30) The CT band of [NCP^+, benzilate] was blue-shifted relative to the corresponding band of the [MV^{2+}, benzilate] ion pair and could not be excited with the femtosecond laser ($\lambda_{exc} > 370$ nm). The experiment thus was carried out with the frequency-tripled output of a 25-ps mode-locked Nd:YAG laser.

(31) (a) The $NCP^\cdot$ radical[31b] has an absorption maximum at $\lambda_{max} = 390$ nm. A band at $\lambda_{max} = 650$ nm, due to intermolecular association, would be too weak to be observed with our apparatus. (b) Itoh, M.; Nagakura, S. *Bull. Chem. Soc. Jpn.* **1966**, *39*, 369.

(32) (a) Johnston, L. J.; Lougnot, D. L.; Wintgens, V. Scaiano, J. C. *J. Am. Chem. Soc.* **1988**, *110*, 518.

(33) Nagarajan, V.; Fessenden, R. W. *Chem. Phys. Lett.* **1984**, *112*, 207.

(34) (a) The ketyl radical of fluorenone has $\lambda_{max} = 520$ nm and $\epsilon_{max} = 1100$ M^{-1} cm^{-1} in aqueous solution.[28] See also: (b) Davidson, R. S.; Santhanam, M. *J. Chem. Soc., Perkin Trans. 2* **1972**, 2355 for its spectrum in various nonaqueous solvents. (c) For the spectrum of the triethylsilyl-substituted analogue, see: Chatgilialoglu, C.; Ingold, K. U.; Scaiano, J. C. *J. Am. Chem. Soc.* **1982**, *104*, 5119.

Table 1. Transient Decays and Quantum Yields of $MV^{+\bullet}$ upon Laser Irradiation of [MV^{2+}, Benzilate] Ion Pairs[a]

benzilate donor[b]	τ_{MV}[c] (ps)	Φ_{MV}[d]
benzilate	no decay	0.79
4,4′-dimethylbenzilate	no decay	0.46
4-methoxybenzilate	2.7	0.28 (0.28)[e]
4,4′-dimethoxybenzilate	1.8	0.24 (0.25)[e]
2,2′,5,5′-tetramethoxybenzilate	1.9	0.05
9-hydroxy-9-fluorenecarboxylate	20	0.05

[a] In aqueous solution at 25 °C. [b] Generated as the sodium salt by dissolution of the free acids in sodium bicarbonate solution. [c] Lifetime of reduced methylviologen ($MV^{+\bullet}$), measured by monitoring the decay of its absorbance at 605 nm following femtosecond laser irradiation. [d] Quantum yield of residual methylviologen at 10 ns following (nanosecond) laser excitation. [e] Quantum yield of $MV^{+\bullet}$ determined 50 ps after excitation in parentheses.

and/or phenyl), the absorption bands of which overlapped with that of $MV^{\bullet+}$. This behavior is labeled **DP** to emphasize the (partial) decay and persistence of the transient species following laser photolysis.

III. Transient Quantum Yields Following Nanosecond Photolysis of [MV^{2+}, $Ar_2C(OH)CO_2^-$] Ion Pairs. The presence of persistent phototransients—$MV^{\bullet+}$ and ketyl radicals—was established by the observation of residual absorptions on the femtosecond/picosecond time scale, as described in section II. To quantify and compare the concentrations of persistent $MV^{\bullet+}$ obtained with the various benzilates in Table 1, we converted the residual absorbances at 605 nm to quantum yields, Φ_{MV}, of persistent $MV^{\bullet+}$ by normalizing them with respect to the light absorbed, i.e., $\Phi_{MV} = [MV^{\bullet+}]_{res}/I_{abs} = A_{res}/\epsilon_{MV}I_{abs}$, where $[MV^{\bullet+}]_{res}$ was the concentration of residual reduced methylviologen, A_{res} the residual absorbance (at 605 nm), ϵ_{MV} the extinction coefficient of reduced methylviologen, and I_{abs} the number of moles of photons absorbed per volume unit.

Two methods were used to determine these quantum yields by laser photolysis experiments. In the first method the residual concentration of $MV^{\bullet+}$ at 50 ps, $A_{50\,ps}/\epsilon_{MV}$, was compared with the concentration of $MV^{\bullet+}$ extrapolated to time zero, A_0/ϵ_{MV}. This extrapolated concentration of $MV^{\bullet+}$ was set equal to I_{abs} by assuming that the radical pair formation in eq 4 occurred with unit efficiency.[35] This gives $\Phi_{MV} = (A_{50ps}/\epsilon_{MV})/(A_0/\epsilon_{MV}) = A_{50ps}/A_0$. This method, however, has problems when applied to the ion pairs with **D** or **P** behavior. Thus, in the case of the kinetic traces with **D** behavior, the measurement of the weak residual absorbance was not sufficiently accurate due to the experimental error (±0.005 absorbance units) in the quantification of the absorbance signals. In the case of **P** behavior, a strong absorbance signal was obtained that did not decay. Extrapolation of this residual absorbance to time zero would result in a unit quantum yield, $\Phi_{MV} = 1.0$. However, such a procedure would overlook any ultrafast decay processes occurring in the time domain of the laser pulse (*vide infra*). In the intermediate (**DP**) cases, the method could be successfully applied, since the absorption band of $MV^{\bullet+}$ decayed to a residual absorbance that was accurately measurable. (See column 3 in Table 1.)

Owing to the restricted applicability of the method described above, a second approach was chosen to determine Φ_{MV} for all the systems (**P**, **D**, and **DP**). Utilizing a slower but more sensitive laser spectrometer based on a Q-switched Nd:YAG laser,[36] we determined the concentration of $MV^{\bullet+}$ at the end of the 10-ns laser pulse and measured the light absorbed (I_{abs}) by transient actinometry.[37] Thus, the CT bands of the various ion pairs in Table 1 were excited with the third harmonic (355 nm) of the laser, and the quantum yields of $MV^{\bullet+}$ (Φ_{MV}) were determined by comparison of its absorbance at 605 nm (A_{MV}) with that of the benzophenone triplet (A_{BP}) monitored at 530 nm.[37] The quantum yields of $MV^{\bullet+}$ in Table 1 decreased smoothly from 0.79 to 0.05 as the donor anion was changed from benzilate to dimethyl-, monomethoxy-, dimethoxy-, and tetramethoxybenzilate. In the cases of **DP** behavior, for which we were able to apply both methods for quantum-yield determination, the values of Φ_{MV} were in good agreement. (See Table 1.) For this reason, we concluded that no significant loss or generation of $MV^{\bullet+}$ occurred between the end of the femtosecond/ picosecond time window (50 ps) and the beginning of the time window of the nanosecond experiment (10 ns).

The absorbance of $MV^{\bullet+}$ on the nanosecond time scale did not remain constant but increased over the interval from 10 to 200 ns. This increase was observed for all the benzilate ions in Table 1, and it was temporally distinct from the initial formation of $MV^{\bullet+}$ on the femtosecond/picosecond time scale. This secondary phase of $MV^{\bullet+}$ production was complete after 200 ns, and the absorbance remained unchanged for time periods exceeding the temporal range (2 ms) of the laser spectrometer. Since the transient quantum yields in Table 1 (Φ_{MV}) were obtained by extrapolating the absorbance traces to zero time, they apply to the primary (femtosecond/picosecond) phase of $MV^{\bullet+}$ production.

In contrast to the diverse kinetic behaviors of the benzilates, the ion pairs formed from MV^{2+} and arylacetates were all characterized by decay of $MV^{\bullet+}$ to the spectral base line, i.e., **D**-type behavior. A clear trend was apparent, however, in the lifetime of $MV^{\bullet+}$, which decreased uniformly as the substituents on the aryl group became more electron-releasing, in the order Cl > H > Ph > OMe. The low quantum yields for persistent $MV^{\bullet+}$, as determined by transient actinometry on the nanosecond time scale (*vide supra*), showed a parallel trend, with Φ_{MV} decreasing along the same sequence as τ_{MV} in Table 2.

IV. Steady-State Photolysis of MV^{2+}/Benzilate Ion Pairs. In general, the degassed aqueous solutions of $MV(OTf)_2$ and the sodium salts of the various benzilate anions, $Ar_2C(OH)CO_2^-$, turned deep blue to indicate the formation of reduced methylviologen, $MV^{\bullet+}$.[22] The blue reaction mixture was extracted with dichloromethane, and GC–MS analysis of the organic extract revealed the formation of the diaryl ketone, Ar_2CO, in accord with previous photodecarboxylation studies.[18] The two photoproducts, $MV^{\bullet+}$ and diaryl ketone, were the only organic products detected in the reaction mixture. In order to clarify the stoichiometry of the reaction these two products were quantified in terms of their photochemical quantum yields.

(35) In accord with the Mulliken formulation of the charge-transfer transition in ref 13.

(36) Bockman, T. M.; Karpinski, Z. J.; Sankararaman, S.; Kochi, J. K. *J. Am. Chem. Soc.* **1992**, *114*, 1970.

(37) (a) Sandros, K. *Acta Chem. Scand.* **1969**, *23*, 2815. (b) Chattopadhyay, S. K.; Kumar, C. V.; Das, P. K. *J. Photochem.* **1985**, *30*, 81. (c) Hurley, J. K.; Sinai, N.; Linshitz, H. *Photochem. Photobiol.* **1983**, *38*, 1.

(38) The ion pair formed from MV^{2+} and tetramethoxybenzilate was an exception, and the orange solution remained unchanged in color even after prolonged irradiation.

Table 2. Transient Decays and Quantum Yields of $MV^{+\bullet}$ upon Laser Irradiation of [MV^{2+}, Arylacetate] Ion Pairs[a]

arylacetate donor	σ^{+} [b]	τ_{MV} [c] (ps)	Φ_{MV} [d]
p-chlorophenylacetate	+0.11	59	0.096
phenylacetate	0.0	39	0.070
4-biphenylacetate	−0.21	15	0.023
p-methoxyphenylacetate	−0.78	4.8	0.007
1-naphthylacetate	−0.3	8.3	<0.005
diphenylacetate		5.5	0.035

[a] In aqueous solution at 25 °C. [b] Hammett coefficient for the aromatic substituent from ref 59b. [c] Lifetime of reduced methylviologen ($MV^{+\bullet}$) measured by monitoring the decay of its absorbance at 605 nm following femtosecond laser irradiation. [d] Quantum yield of residual methylviologen 10 ns after laser irradiation.

Table 3. Steady-State Photochemical Quantum Yields for the Reaction of MV^{2+} with substituted Benzilates[a]

benzilate anion	Φ_{SS} [b]	Φ_{aer} [c]	Φ_{cat} [d]
benzilate	1.14	0.78	0.71
4,4′-dimethylbenzilate	0.96	0.55	0.52
4-methoxybenzilate	0.47	0.23	0.29
4,4′-dimethoxybenzilate	*e*	0.26	0.20
2,2′,5,5′-tetramethoxybenzilate	<0.01	<0.03	*e*

[a] In aqueous solution at 25 °C using the 366-nm light of a mercury lamp as irradiation source. [b] Photochemical quantum yield of $MV^{+\bullet}$ in deaerated solution, as determined by UV−vis spectroscopy. [c] Photochemical quantum yield of diaryl ketone in aerated solution, as determined by GC analysis. [d] Photochemical quantum yield of diaryl ketone in the presence of platinum dioxide (see text) as determined by GC analysis. [e] Not measured.

The light source for the steady-state experiments was the 366-nm emission of a medium-pressure mercury lamp, and the light flux was determined by actinometry using Aberchrome-540 according to the procedure of Heller and Langan.[39] The formation of $MV^{+\bullet}$ was quantified by UV−vis spectrophotometry. The steady-state quantum yields (Φ_{SS}) for the formation of $MV^{+\bullet}$ are listed in Table 3. A comparison of the transient yields, Φ_{MV} in Table 1, with the steady-state yields, Φ_{SS} in Table 3, shows that Φ_{SS} was consistently greater than Φ_{MV} in all cases by a factor of about 2.

Attempts to measure the photochemical quantum yields for ketone formation were not successful in degassed solutions. Photochemical conversion of the benzilate anion to the diaryl ketone remained low even after prolonged periods (several hours) of irradiation. We concluded that the photogenerated $MV^{+\bullet}$ absorbed the actinic light, and this "inner filter" effect[40,41] prevented efficient photolysis. To overcome this problem, two methods were devised to remove the interfering $MV^{+\bullet}$ by chemical means. In the first method, the photolysate was continuously purged with air to provide a constant concentration of dissolved dioxygen. Since $MV^{+\bullet}$ reacts quantitatively with O_2,[42] i.e.,

$$MV^{+\bullet} + O_2 \rightarrow MV^{2+} + O_2^{-\bullet} \quad (7)$$

the buildup of $MV^{+\bullet}$ was prevented. The second approach relied on the catalyzed reaction of $MV^{+\bullet}$ with H^+ in the aqueous medium.[43,44] Platinum dioxide (Adams catalyst) was added to the reaction mixture prior to photolysis, so that photogenerated $MV^{+\bullet}$ was consumed by the redox reaction

$$2MV^{+\bullet} + 2H^+ \xrightarrow{[PtO_2]} 2MV^{2+} + H_2 \quad (8)$$

Indeed, the presence of either O_2 or PtO_2 in the reaction mixture completely eliminated the accumulation of $MV^{+\bullet}$, and the solutions did not develop the characteristic blue coloration of the reduced viologen throughout the irradiation period. Irradiation times were limited to 60−80 min, and conversions were kept low in order to minimize reactions of MV^{2+} or $Ar_2C(OH)CO_2^-$ with $O_2^{\bullet-}$ or H_2 formed in eqs 7 and 8. The photochemical yields of Ar_2CO were determined by means of gas chromatography, with 4-chlorobenzophenone as the internal standard. The quantum efficiencies for the formation of ketones in the aerated and catalyzed reactions are listed in Table 3 as Φ_{aer} and Φ_{cat}, respectively.

Three observations should be emphasized with regard to the quantum yields in Table 3: (1) The photochemical quantum yields of diaryl ketone are the same in both the catalyzed (Φ_{cat}) and the aerated (Φ_{aer}) reactions. (2) The formation of diaryl ketone is approximately one half as efficient as the steady-state formation of $MV^{+\bullet}$ (Φ_{ss}). (3) The *photochemical* quantum yields for ketone formation (Φ_{aer} or Φ_{cat}) are identical to the *transient* yields of $MV^{+\bullet}$ (Φ_{MV}). (Compare Tables 1 and 3.)

Discussion

Charge-transfer irradiation of [MV^{2+}, $Ar_2C(OH)CO_2^-$] ion pairs results in efficient oxidative decarboxylation of the benzilate anion, and the scission of the C−CO_2 bond leads to diaryl ketones as the ultimate products. To clarify the course of this reaction, and, particularly, to focus on the intermediate cleavage step, we first determine the overall stoichiometry of this transformation. The femtosecond/picosecond reaction dynamics subsequent to charge-transfer excitation is then analyzed in terms of the observed **P**, **D**, and **DP** kinetic behaviors. Finally, the relationship between the rate and efficiency of the cleavage processes and the structures of the carboxylate donors will be explored.

I. Stoichiometry of the Photoredox Reactions of [MV^{2+}, Benzilate] Ion Pairs. Charge-transfer photolysis of the ion pairs formed from methylviologen dication (MV^{2+}) and benzilate anion ($Ph_2C(OH)CO_2^-$) yields the reduced form of the viologen acceptor ($MV^{+\bullet}$) and benzophenone as products. Formally, the decarboxylation of benzilate to produce benzophenone is a *two-electron* oxidation,

$$Ph_2C(OH)CO_2^- \xrightarrow{-2e} Ph_2CO + CO_2 + H^+ \quad (9)$$

whereas the reduction of the methylviologen dication is a one-electron-transfer step, i.e.

(39) Heller, H. G.; Langan, J. R. *J. Chem. Soc., Perkin Trans. 2* **1981**, 341. See also: Kuhn, H. J.; Braslavsky, S. E.; Schmidt, R. *Pure Appl. Chem.* **1989**, *61*, 187.

(40) Eaton, D. R., in *CRC Handbook of Photochemistry*, Vol 1; Scaiano, J. C., ed; CRC Press: Boca Raton, FL, 1989, p. 1233.

(41) The intense absorption of reduced methylviologen[22] allows quantities of $MV^{+\bullet}$ as small as 0.1 μmol to be assayed after short (1 min) irradiation times. Under these conditions, the formation of the byproduct diaryl ketone (0.05 μmol) would be too small to be reliably quantified. As a result, the ratio of the quantum yields for formation of reduced methylviologen and of diaryl ketone could not be determined under the same conditions of photolysis. [Continued irradiation was unproductive, since the photogenerated $MV^{+\bullet}$ absorbed more than 90% of the incident actinic light and the reaction effectively ceased.]

(42) (a) Rodgers, M. A. J. *Radiat. Phys. Chem.* **1984**, *23*, 245. (b) Tsukuhara, K. Wilkins, R. G. *J. Am. Chem. Soc.* **1985**, *107*, 2632.

(43) Kalyanasundaram, K.; Kiwi, J.; Grätzel, M. *Helv. Chim. Acta* **1978**, *61*, 2720.

(44) Harriman, A.; West, M. A. *Photogeneration of Hydrogen*; Academic: New York, 1982.

$$MV^{2+} \xrightarrow{+e} MV^{\bullet+} \quad (10)$$

A comparison of the quantum yields for the formation of $MV^{\bullet+}$ ($\Phi_{ss} \approx 1.2$) and of benzophenone ($\Phi_{aer} \approx \Phi_{cat} \approx 0.8$) in Table 3 indicates that $MV^{\bullet+}$ and benzophenone are formed in an approximate 2:1 ratio. Similar ratios prevail in the reactions of other (substituted) benzilate anions, $Ar_2C(OH)CO_2^-$, with $MV^{2\bullet+}$ The experimental ratios of the quantum yields in Table 3 point to an overall 2:1 stoichiometry, *i.e.*,

$$2MV^{2+} + Ar_2C(OH)CO_2^- \xrightarrow{h\nu_{CT}} 2MV^{\bullet+} + Ar_2CO + CO_2 + H^+ \quad (11)$$

to accord with the formal stoichiometry that results from the combination of eqs 9 and 10. The time-resolved measurements show that the 2 equiv of reduced methylviologen are formed in distinct steps on the femtosecond and on the nanosecond time scales, respectively. The first of these processes is the photoinduced electron transfer in eq 4 to generate the [$MV^{\bullet+}$, $Ar_2C(OH)CO_2^{\bullet}$] radical pair. The second process is the oxidation of the ketyl radical by MV^{2+}, *i.e.*,

$$MV^{2+} + Ar_2C(OH)^{\bullet} \rightarrow MV^{\bullet+} + Ar_2CO + H^+ \quad (12)$$

as originally suggested by Barnett *et al.*[18] (Ketyl radicals are oxidized by MV^{2+} with rate constants on the order of 10^8 M^{-1} s^{-1}.[45]) The crucial step linking the photoinduced electron transfer in eq 4 to the formation of the diaryl ketone in eq 12 is the decarboxylation of the acyloxy radical, $Ar_2C(OH)CO_2^{\bullet}$. Consequently, we concentrate on the steps immediately following the electron transfer in eq 4, particularly the C−C bond cleavage implied by the formation of diaryl ketone (eq 11).

II. Femtosecond/Picosecond Dynamics of [$MV^{\bullet+}$, Acyloxy] Radical Pairs. The spectroscopic observation of benzophenone ketyl radical (Figure 2) within a picosecond of laser excitation of the ion pair in eq 5 clearly demonstrates the rapid cleavage of the $C-CO_2$ bond in the benziloxy radical. However, the picosecond decays in Figures 4 and 5, combined with the quantum yields of less than unity in Tables 1 and 3, point to the existence of a competing back-electron transfer process to restore the original CT-ion pair. Back-electron transfer is ubiquitous in photoinduced redox processes, and it typically dominates the reactivity of the radical pairs generated by charge-transfer excitation.[14−16] The various dynamic behaviors of the $MV^{\bullet+}$/acyloxy radical pairs illustrated in Figures 2−5 can be simply analyzed in terms of this competition between carbon−carbon bond cleavage (k_{CC}) and back-electron transfer (k_{bet}) as depicted in Scheme 1.

The scission of the $R-CO_2$ bond yields a triad of $MV^{\bullet+}$, CO_2, and the radical, $R^{\bullet}$, while the competing back-electron transfer restores the original CT ion pair. Diffusive separation of the radical pair is not considered explicitly in Scheme 1 since the rapidity of the chemical transformations (k_{CC} and k_{bet}) of the benziloxy radicals

Scheme 1

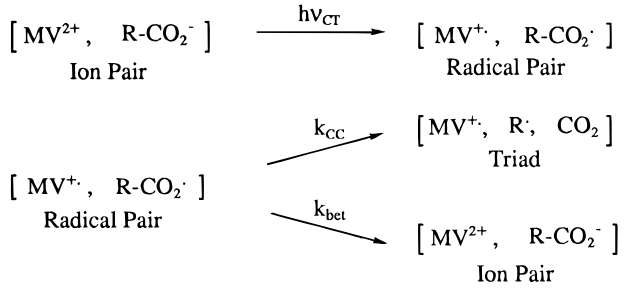

R = $Ar_2C(OH)$ or $ArCH_2$

(which are complete in 10 ps) does not allow diffusive separation to compete.[46]

The various kinetic behaviors of the [$MV^{\bullet+}$, benziloxy] radical pairs, *i.e.*, **P**, **D**, and **DP**, can be described in terms of the competing processes in Scheme 1. **P-Behavior:** For the parent [MV^{2+}, $Ph_2C(OH)CO_2^-$] ion pair, the ketyl radical intermediate is observed within 1.0 ps of the laser pulse (Figure 2). Decarboxylation (k_{CC}) thus occurs very rapidly, and it successfully competes with back-electron transfer (k_{bet}). As a result, high quantum yields (both steady-state and transient) for the formation of reduced methylviologen and benzophenone are obtained. (See Tables 1 and 3.) **D-Behavior:** By contrast, the radical pair derived from 2,2′,5,5′-tetramethoxybenzilate and MV^{2+} undergoes back-electron transfer (k_{bet}) predominantly, as indicated by the absence of the ketyl radical as a spectral transient in Figure 4 and the smooth decay of the absorbance of $MV^{\bullet+}$ to the spectral base line. The yields of photoproducts in this case are negligible. **DP-Behavior:** In the radical pairs derived from MV^{2+} and monomethoxy- and dimethoxybenzilate, the competing processes of bond scission (k_{CC}) and back-electron transfer (k_{bet}) occur with comparable probabilities. Accordingly, the femtosecond spectral transients decay partially to a non-zero base line, and intermediate values of the quantum yields are obtained. In summary, the various femtosecond/picosecond kinetic behaviors (**P**, **D**, and **DP**) are explained in qualitative terms by the simple competition between decarboxylation (k_{CC}) and back-electron transfer (k_{bet}) as depicted in Scheme 1. However, both of these processes occur in the same time domain as the photoactivation of the CT ion pair. Thus, a complete quantitative simulation of the radical pair dynamics requires the explicit inclusion of the temporal profile of the laser excitation process.

We first consider the rise and decay of reduced methylviologen for the simplest case, considering only the back-electron-transfer pathway (i.e., $k_{bet} \gg k_{CC}$ in Scheme 1). The mathematical description of the kinetics in this case is given by the convolution of the experimental decay (k_{bet}) with the laser pulse (τ), as described in the Experimental Section.[47,48] Figure 6 shows the simulated kinetic traces for the absorbance of $MV^{\bullet+}$ (A_{MV}) as a function of k_{bet}. As the value of k_{bet} increases, the temporal behavior of the absorbance changes from an

(45) (a) Small, R. D.; Scaiano, J. C. *J. Photochem.* **1977**, *6*, 453. (b) Ketyl radicals are electron rich by virtue of their very low oxidation potentials and ease of oxidation in solution. See: (c) Baumann, H.; Merckel, C.; Timpe, H.-J.; Graness, A.; Kleinschmidt, J.; Gould, I. R.; Turro, N. J. *Chem. Phys. Lett.* **1984**, *103*, 497. (d) Kemp, T. J.; Martins, L. J. A. *J. Chem. Soc., Perkin Trans. 2* **1980**, 1708. (e) Engel, P. S.; Wu, W. X. *J. Am. Chem. Soc.* **1989**, *111*, 1830.

(46) The escape of the benziloxy radicals out of the solvent cage is not included in the femtosecond kinetics, since it occurs on much slower time scales. See: Scott, T. W.; Liu, S. N. *J. Phys. Chem.* **1989**, *93*, 1393. (b) Cage escape may compete with the slower reactions of the [$MV^{\bullet+}$, arylacetoxy] radical pairs.

(47) Compare: Peters, K. S.; Li, B. *J. Phys. Chem.* **1994**, *98*, 401.

(48) Asaki, M. T.; Huang, C.-P.; Garvey, D.; Zhou, J.; Kapteyn, H. C.; Murnane, M. M. *Opt. Lett.* **1993**, *18*, 977.

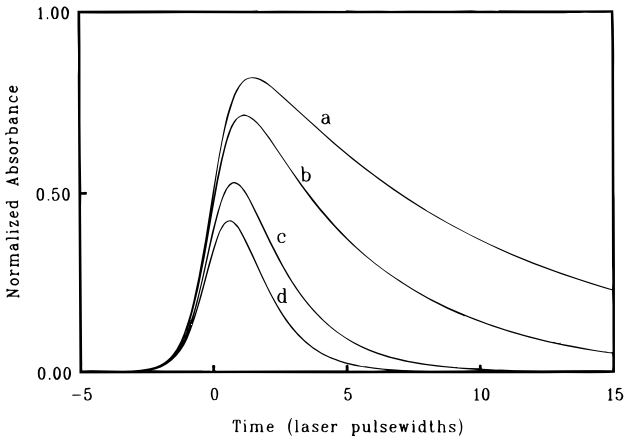

Figure 6. Simulation of **D**-behavior for various values of k_{bet} (in reciprocal laser pulsewidths, τ^{-1}): (a) 0.1, (b) 0.2, (c) 0.5, and (d) 1.0.

exponential decay (curve a in Figure 6) to a symmetrical rise and fall that closely follows the temporal profile of the laser pulse (curve d). In addition to the change in shape, we call attention to the diminution of the maximum value of A_{MV} as k_{bet} increases. Despite the variations in the size and shape of the temporal responses, all of the simulated traces reach the spectral base line. These simulated kinetic behaviors thus correspond to the decay-dominated kinetics (**D**-type) of the radical pairs in Table 1.

If the cleavage reaction in Scheme 1 is to be included in the kinetics (i.e., if $k_{CC} \approx k_{bet}$), it is convenient to define an *overall* decay rate constant, k, and a partition ratio, R, in terms of the rate constants for decarboxylation and back electron transfer.

$$k = k_{bet} + k_{CC} \tag{13}$$

$$R = k_{CC}/(k_{bet} + k_{CC}) \tag{14}$$

These parameters, k and R, are varied to generate the family of simulated traces in Figure 7. In Figure 7A the time-dependent absorptions of $MV^{\bullet+}$ are shown for a fixed value of k (10^{12} s^{-1}) and for varying partition ratios, R. For $R = 0.05$ (curve a), the simulated absorbance decays nearly to the base line and thus approximates **D**-behavior. On the other hand, a R value of 0.8 results in a rise with no apparent decay component, to simulate **P**-behavior (curve d). (Note that R need not be unity to yield simulations of a simple rise to a nondecaying plateau.) The intermediate values of R lead to a rise and decay to a raised base line, in accordance with **DP** behavior (curves b and c).

In the case of partial decay (**DP** behavior), the shape of the temporal profile of $MV^{\bullet+}$ absorbance is sensitive not only to R, but also to the overall rate constant, k. Figure 7B shows the changes in the simulated absorbance profiles at a fixed value of $R = 0.5$ and variable k. As k approaches the time constant of the laser pulse (τ^{-1}), the decay component in the traces becomes less pronounced. Ultimately, this leads to a kinetic profile consisting of a simple rise to a persisting plateau (**P** behavior) at $k = 2\tau^{-1}$. In other words, **P**-behavior can be explained either by a fast decarboxylation rate compared with back-electron transfer ($k_{CC} \gg k_{bet}$) or by comparable rates ($k_{CC} \approx k_{bet}$) combined with overall fast kinetics ($k_{CC} + k_{bet} \approx \tau^{-1}$). (Compare curve d in Figure 7A with curve c in Figure 7B.) In summary, the full range of kinetic behaviors (**P**, **D**, and **PD**) can be simulated using the simple kinetics of Scheme 1, with only two adjustable parameters, k and R. The simulation parameters, k and R, can now be related to experimentally observed quantities, i.e., the picosecond decays (τ_{MV}) and the transient quantum yields (Φ_{MV}). The partition ratio, R, as defined in eq 14, reflects the extent to which reduced methylviologen escapes back-electron transfer to appear in the triad. Thus, R is equal to Φ_{MV}, the transient quantum yield of reduced methylviologen. Since all the kinetic behaviors can be simulated by varying R and k (see above), and since R is experimentally determined as Φ_{MV}, one can now fit the simulated absorbance profiles to the experimental data by adjusting one single parameter, k. Figure 8 shows fits of the absorbance of $MV^{\bullet+}$ to the simulated curves. The k and R values may now be used to calculate the values of the rate constants k_{bet} and k_{CC} for ion pairs that show **D** or **DP** behavior according to eqs 13 and 14 (see Table 4).

For the benzilate ion pair, which shows **P**-behavior, k_{CC} can be obtained from the growth kinetics of the absorbance of the $Ph_2C(OH)^{\bullet}$ radical, since the rise of its absorbance depends on k_{CC} in Scheme 1, while the rise of $MV^{\bullet+}$ depends only on the pulse width. We observed a significant time lag of 2−3 ps between the formation of $MV^{\bullet+}$ (monitored at 605 nm) and the slower formation of $Ph_2C(OH)^{\bullet}$ (monitored at 530 nm). (See the inset to Figure 2.) The best fit for the rise of the 530-nm absorbance was obtained for $k_{CC} = 8 \times 10^{11}$ s^{-1} in Figure 8C. (See the Experimental Section for the details of this analysis.) Consequently, k_{bet} must have a value of 2×10^{11} s^{-1} to accommodate the observed quantum yield, $\Phi_{MV} = R = 0.79$ in eq 14. For the ion pair derived from 4,4′-dimethylbenzilate, the rate constants, k_{CC} and k_{bet}, could not be determined in this way, since there was no measurable time lag between the rise of the ketyl radical and the rise of $MV^{\bullet+}$. A lower limit for k can, however, be estimated from the transient quantum yield Φ_{MV}. To successfully simulate the observed **P** behavior of this ion pair with an observed R value (Φ_{MV}) of 0.46, it is necessary to choose k in eq 13 to be greater than 10^{12} s^{-1}. (Note that this represents a case in which there is no apparent decay even though R is considerably less than unity.) On the basis of these values of R and k we estimate that $k_{CC} \approx k_{bet} \geq 5 \times 10^{11}$ s^{-1}.

Scheme 1 can also be applied to the radical pairs formed by photolysis of arylacetate CT-ion pairs. Since these decay rates are all substantially slower than the laser pulse, the kinetics of the excitation need not be taken into account. The observed first-order decay constant is thus equal to k, and the values of Φ_{MV} in Table 2 can be equated to R. The rate constants for back-electron transfer and C−C bond cleavage in Table 5 were thus extracted from the picosecond decays and transient quantum yields of reduced methylviologen according to eqs 13 and 14.

III. Trends in the Rates of Decarboxylation and Back-Electron Transfer. The most remarkable observation in this study is the extremely rapid fragmentation of benziloxy radicals. The rate constants for carbon−carbon bond cleavage in Table 4, which are on the order of 10^{12} s^{-1}, approach those of barrier-free unimolecular reactions, for which rate constants of 10^{13} s^{-1} are calcu-

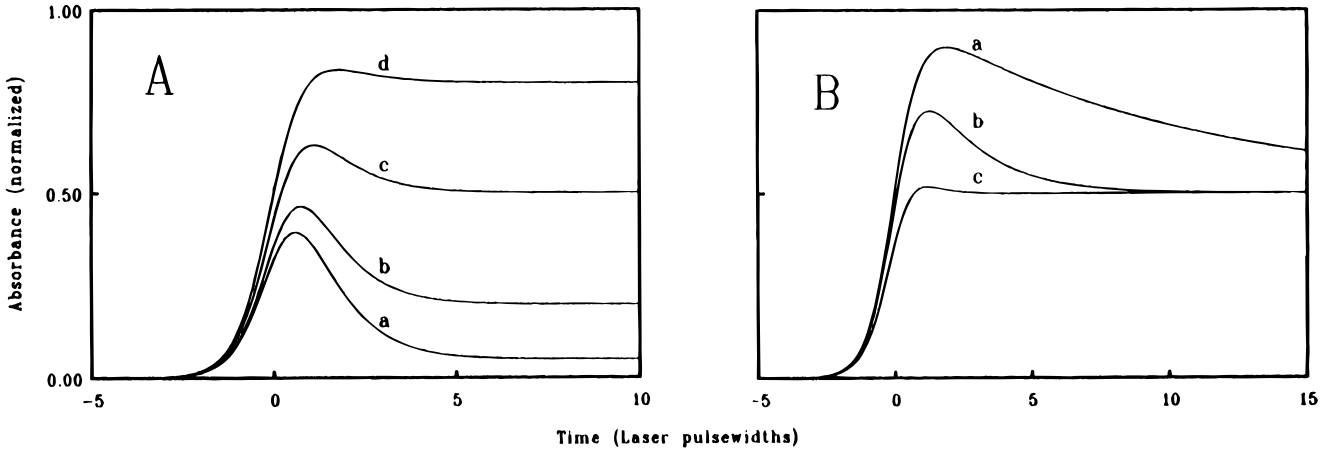

Figure 7. Simulation of **DP**-behavior for various values of k and R. **A**: $k = 1.0$ reciprocal laser pulsewidths and $R =$ (a) 0.05, (b) 0.2, (c) 0.5, and (d) 0.8. **B**: R = 0.5 and $k =$ (a) 0.2, (b) 1.0, and (c) 2.0 reciprocal laser pulsewidths.

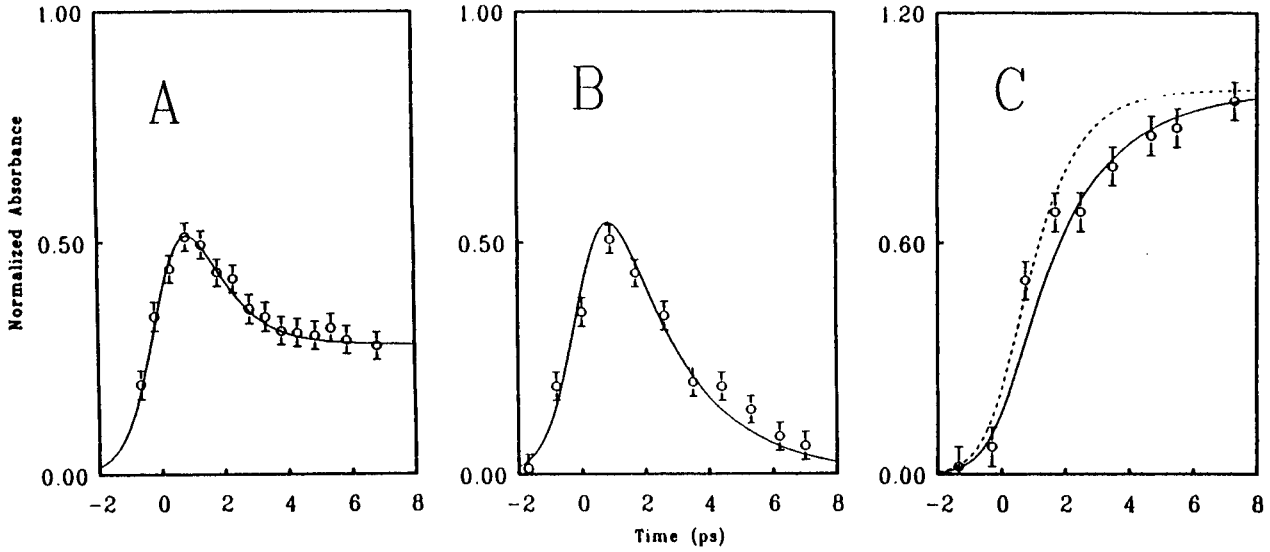

Figure 8. Experimental data for the normalized absorbance of $MV^{\bullet+}$ (large open circles) superimposed on simulated kinetic traces. A: MV^{2+}/4,4′-dimethoxybenzilate, simulated as **DP** -behavior, with $k = 1.0 \times 10^{12}$ s^{-1} and $R = 0.24$. B: MV^{2+}/2,2′,5,5′-tetramethoxybenzilate, simulated as **D**-behavior, with $k = 8.3 \times 10^{11}$ s^{-1} and $R = 0.05$. C: MV^{2+}/benzilate, simulated as **P** -behavior, with $k_{CC} = 8 \times 10^{11}$ s^{-1}; the dotted line shows the simulated response of the laser system. Error bars represent experimental errors of 10% of the maximum absorbance.

Table 4. Rate Constants for Decarboxylation and Back Electron transfer in Methylviologen/Benzilate Ion Pairs[a]

benzilate donor	k_{bet}[b] (10^{11} s^{-1})	k_{CC}[c] (10^{11} s^{-1})
benzilate	2	8
4,4′-dimethylbenzilate	5[d]	5[d]
4-methoxybenzilate	3	1
4,4′-dimethoxybenzilate	8.0	2.0
2,2′,5,5′-tetramethoxybenzilate	8.3	0.4
9-hydroxy-9-fluorenecarboxylate	0.48	0.02

[a] Calculated using eqs 13 and 14. [b] Rate constant for back-electron transfer within the radical pair in Scheme 1. [c] Rate constant for decarboxylation of the acyloxy radical derived from the benzilate anion in column 1. [d] Lower limit; see text.

Table 5. Rate Constants for Decarboxylation and Back-Electron Transfer in Methylviologen/Arylacetate Ion Pairs[a]

arylacetate	k_{bet}[b] (10^{11} s^{-1})	k_{CC}[c] (10^{9} s^{-1})
p-chlorophenylacetate	0.15	1.6
phenylacetate	0.26	1.8
4-biphenylylacetate	0.64	1.5
p-methoxyphenylacetate	2.1	1.5
1-naphthylacetate	1.2	<0.2
diphenylacetate	1.7	6.1

[a] Calculated using eqs 13 and 14. [b] Rate constant for back-electron transfer from reduced methylviologen to the acyloxy radicals derived from the arylacetate anions in column 1. [c] Rate constant for decarboxylation of the acyloxy radical.

lated.[49] These rapid rates imply that the benziloxy radicals are separated from the transition states for C−C bond cleavage by activation barriers of only 1−2 kcal mol^{-1}.[50] The ultrafast decarboxylation of $Ar_2C(OH)CO_2^{\bullet}$ should be contrasted with the relatively slower rate ($k_{CC} = 1-2 \times 10^9$ s^{-1}) that pertains to the arylacetoxy radicals in Table 5. The latter are within the range of previously reported values[8-11] of k_{CC} determined for various aliphatic acyloxy radicals. The ultrafast rates of decarboxylation of the benziloxy radicals are dependent on the substituents in the aromatic ring, with electron-donating substituents inducing a diminution in k_{CC}. The ultrafast rates may be rationalized on the basis of the reaction

(49) Moore, J. W.; Pearson, R. G. *Kinetics and Mechanism*, 3rd ed.; Wiley: New York, 1981, p 173.
(50) Calculated by means of the Eyring equation in ref 49.

energetics, while the substituent effects point to the influence of electronic factors.

Reaction Energetics. Although decarboxylation of aliphatic acyloxy radicals (R = alkyl in eq 1) is exergonic,[51] theoretical and experimental studies agree that the loss of carbon dioxide requires a significant activation energy.[52] *Ab initio* calculations indicate that decarboxylation corresponds to an intended crossing of the π ground state with low-lying σ states of the acyloxy radical.[52] Accordingly, the increasing stability of R$^\bullet$ in eq 1 lowers the barrier to C−C bond scission by moving the crossing point closer to the reactant surface. Thus, the increased stability of ketyl radicals, $Ar_2C(OH)^\bullet$, relative to benzyl radicals, $ArCH_2^\bullet$, implies a lowering of the transition-state free energy ($\Delta G^\ddagger$) for the decarboxylation of the corresponding benziloxy radicals.[53] The transition state for this decarboxylation is lower in energy (relative to those of arylacetoxy radicals) owing to more extensive delocalization (over two aromatic rings rather than one) of the radical center that is forming on the benzilic carbon during the decarboxylation.

Substituent Effects. As shown in Table 4, decarboxylation rates decrease systematically as electron-donating groups are added to the aromatic system. Thus, the unsubstituted benziloxy radical decarboxylates at ultrafast rates, while its dimethoxy-substituted analogue fragments four times more slowly. Additional methoxy substitution (to form tetramethoxybenzilate) results in a further 5-fold decrease in k_{CC}. To explain this effect, let us consider the critical intermediate, the benziloxy radical $Ar_2C(OH)CO_2^\bullet$, which can be thought of as either a zwitterionic species, consisting of an arene cation radical with a remote carboxylate substituent (**I**), or as a simple acyloxy radical with the unpaired electron centered on the carboxyl group (**II**). The relative contributions of structures **I** and **II** are controlled by the distribution of electron density over the benziloxy radical, which in turn depends on the substituents on the aromatic ring.[54] Electron-releasing groups (G) will stabilize **I** more than **II**. Since structure **I**, with an anionic carboxyl group, is less prone to loss of CO_2 than structure **II**, which contains an acyloxy group, the presence of electron-donating substituents will disfavor decarboxylation.[55] This "trapping" of the electron deficiency within the aromatic π-system (as illustrated in structure **I**) also explains the anomalously low rates of decomposition of the acyloxy radicals derived from hydroxyfluorenecarboxylate and naphthylacetate. (See entries 6 in Table 1 and 5 in Table 2.) In both of these cases, the cation radical structure analogous to **I** (for which decarboxylation is not favorable) is strongly preferred, since the positive charge is delocalized over an extended aromatic system.

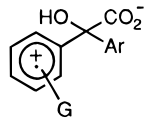

I

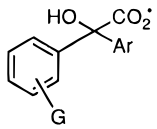

II

The C−C bonds of the acyloxy radicals derived from substituted phenylacetates are cleaved with a uniform rate constant of $k_{CC} = 1.6 \pm 0.3 \times 10^9$ s^{-1}, regardless of the substituents on the phenyl ring. (See entries 1−4 in Table 5.) The nonvariant decarboxylation rates of these $ArCH_2CO_2^\bullet$ radicals are in accord with indirect measurements of the decarboxylation of a series of substituted acyloxy radicals, which have cleavage rate constants, k_{CC}, between 1 and 11×10^9 s^{-1}.[57] These relatively slow rates imply higher activation barriers for decarboxylation, which in turn points to a strengthening of the C−CO_2 bonds of the arylacetoxy radicals relative to their benziloxy counterparts. Thus, we conclude that the remote substituent effect is only pronounced for the cleavage of the very weak C−C bonds of $Ar_2C(OH)CO_2^\bullet$ and not for the relatively stronger ones of $ArCH_2CO_2^\bullet$.

Back-Electron Transfer. The rate constants for back-electron transfer (k_{bet}) in Tables 4 and 5 increase monotonically as the aromatic nuclei in the carboxylate donors are substituted with electron-releasing groups, in the order phenyl < methyl < methoxy. For the benzilates, this trend extends over a factor of 4 in k_{bet} proceeding from benzilate to tetramethoxybenzilate. (See Table 4.) An even clearer tendency is apparent for the arylacetate donors, as reflected in an increase of more than 1 order of magnitude as the *para* substituent is changed from chloro to hydrogen, phenyl, and methoxy. (See Table 5.) The trend is correlated with the increasing donor strength of the substituent, as assessed by the decreasing values of the Hammett parameter, σ^+,[58,59] and also follows the increasing red-shift of the charge-transfer absorption bands. This spectral shift relates directly to the decreasing oxidation potentials ($E°_{ox}$) of the carboxylate donors[13] and thus to the decreasing driving force, $-\Delta G_{bet} = F(E°_{ox} + E°_{red})$ for the back-electron transfer in Scheme 1. ($E°_{red}$ represents the reduction potential of the methylviologen acceptor and F the Faraday constant of 23.1 kcal mol^{-1} V^{-1}.) Thus, the decreased exergonicity for the electron-transfer process is accompanied by an increase in k_{bet}.[60] Such a free energy correlation is termed "inverted" to contrast with the "normal" behavior of increasing reaction rate with increasing thermodynamic driving force. The inverted

(51) (a) Edge, D. J.; Kochi, J. K. *J. Am. Chem. Soc.* **1973**, *95*, 2635. (b) Benassi, R.; Taddei, F. *Tetrahedron* **1994**, *50*, 4795.

(52) Pacansky, J.; Brown, D. W. *J. Phys. Chem.* **1983**, *87*, 1553.

(53) In this context, the enhanced rate for the loss of CO_2 from the diphenylacetoxy radical ($k_{CC} = 6.1 \times 10^9$ s^{-1}) relative to that from phenylacetoxy (1.6×10^9 s^{-1}) results in a similar (though less pronounced) effect (see Table 5).

(54) The radical is conceived of as a resonance hybrid of structures **I** and **II**. The possibility that **I** and **II** are distinct chemical species and that there is a chemical transformation prior to decarboxylation seems unlikely at this juncture (since **I** and **II** differ only in their electronic configuration) but cannot be ruled out *a priori*. Note that the distinction between nuclear and electronic motion becomes difficult to draw as the time scale of fast (fs) reactions approaches the time domain for electronic redistribution.[56]

(55) The effect of electron-withdrawing substituents such as chloro could not be examined, since the charge-transfer absorption band of the [MV^{2+}, 4,4′-dichlorobenzilate] ion pair was blue-shifted to λ_{CT} < 360 nm and thus could not be excited with the Ti:sapphire laser.

(56) (a) Schlag, E. W.; Schneider, S.; Fischer, S. *Ann. Rev. Phys. Chem.* **1971**, *22*, 465. (b) Kompa, K. L.; Levine, R. D. *Acc. Chem. Res.* **1994**, *27*, 91.

(57) The minor discrepancy between the values of k_{CC} for decarboxylation of $PhCH_2CO_2^\bullet$ obtained by Hilborn and Pincock (5×10^9 s^{-1}) in methanol[10] and by us (1.6×10^9 s^{-1}) in water may be due to a solvent effect, since decarboxylations are slower in polar than in nonpolar solvents.[11c] Alternatively, the rate of the clock reaction used by these authors (decarboxylation of the 9-methylfluorenecarboxyl radical) may be somewhat overestimated. (See footnote 20 in ref 9.)

(58) The linear free-energy relation yields $\rho^+ = -1.73$ for the back-electron transfer.

(59) (a) Brown, H. C.; Okamoto, Y.; Inukai, T. *J. Am. Chem. Soc.* **1958**, *80*, 4964. (b) Taylor, R. *Electrophilic Aromatic Substitution*; Wiley: New York, 1990; p 455f.

(60) (a) Marcus, R. A. *Annu. Rev. Phys. Chem.* **1964**, *15*, 155. (b) Marcus, R. A. *J. Chem. Phys.* **1965**, *43*, 679. (c) Marcus, R. A. *Faraday Discuss. Chem. Soc.* **1982**, *74*, 7. (d) Marcus, R. A. *J. Chem. Phys.* **1956**, *24*, 966.

trend in k_{bet} is in accord with previous studies of back-electron transfer within EDA complexes composed of a variety of neutral and charged donors and acceptors.[14,61,62] In particular, inverted behavior applies to back-electron transfer within complexes of methylviologen with both neutral and anionic donors.[62] The driving force dependency of k_{bet} in MV^{2+}/carboxylate ion pairs is thus qualitatively the same as that observed with other methylviologen EDA complexes. In addition the range of k_{bet} in Tables 4 and 5 is the same (10^9-10^{11} s^{-1}) as has been observed for other radical pairs containing $MV^{\bullet+}$.[62] Thus, the distinction between the dissociative and non-dissociative processes is not reflected in the rates of back-electron transfer.[63]

In summary, the diverse efficiencies for decarboxylation within radical pairs derived from benzilate donors results from competing reactions, the decarboxylation of the acyloxy radicals, $Ar_2C(OH)CO_2^{\bullet}$, and back-electron transfer. The former process is retarded and the latter enhanced by electron-rich substituents. In the case of the arylacetoxy radicals, on the other hand, the variation in the decarboxylation efficiency is governed solely by the rate of electron transfer, since k_{CC} is invariant.

Conclusions

CT ion pairs formed from methylviologen (MV^{2+}) and substituted arylacetate or benzilate anions transfer an electron from the carboxylate donor to MV^{2+} upon charge-transfer irradiation. The acyloxy radical in the photogenerated radical pair, [$MV^{\bullet+}$, $RCO_2^{\bullet}$], rapidly loses carbon dioxide by cleavage of the $C-CO_2$ bond. Back-electron transfer to restore the original ion pair competes with this process. Time-resolved spectroscopy on the femtosecond and nanosecond time scales allows the two reaction pathways to be directly observed and quantified.

Decarboxylation rate constants for arylacetoxy radicals lie in the range of 10^9 s^{-1} and, thus, are in agreement with values reported previously.[10] In contrast, the rate constant for cleavage of the benziloxy radical is on the order of 10^{12} s^{-1}. The high stability of the product radical, $Ph_2C(OH)^{\bullet}$, effects a decrease in the activation energy, which in turn leads to ultrafast rates of carbon−carbon bond cleavage. The cleavage rates are modulated by the electronic effects of substituents on the aromatic rings, with electron-withdrawing groups enhancing the rate of $C-CO_2$ scission. By manipulation of these structural factors, it should be possible to design carboxylate donors that lose an electron and cleave the C−C bond in a single step. In such concerted electron-transfer/bond-cleavage reactions the transition state will be directly generated and observed.

Experimental Section

Materials. Phenylacetic acid, *p*-chlorophenylacetic acid, *p*-methoxyphenylacetic acid, and 4-biphenylylacetic acid were obtained from Aldrich and used as received. 1-Naphthylacetic acid, 9-hydroxy-9-fluorenecarboxylic acid, and 9-fluorenecarboxylic acid (Aldrich) were recrystallized from water and dried at 60 °C *in vacuo*. Diphenylacetic acid and benzilic acid (Aldrich) were used as received.

Synthesis of Benzilic Acids. The substituted benzilic acids used in this study were prepared by rearrangement of the corresponding benzils using potassium hydroxide in *n*-butyl alcohol, according to the procedure of Ford-Moore,[65] and were recrystallized from a mixture of ethyl acetate and hexanes. **4,4′-Dimethylbenzilic Acid.** From 4,4′-dimethylbenzil[66] in 58% yield: mp 128−129 °C (lit.[67] mp 127−129 °C); ^{1}H-NMR (acetone-d_6) δ 7.36 (d, J = 8.1 Hz, 4H), 7.07 (d, J = 8.1 Hz, 4H), 5.3 (br, 2H), 2.30 (s, 6H); ^{13}C-NMR (acetone-d_6) δ 175.5, 141.2, 137.8, 129.1, 128.4, 81.1, 21.1. **4-Methoxybenzilic Acid.** From 4-methoxybenzil[66] in 35% yield: mp 143−144 °C (lit.[66] mp 147 °C); ^{1}H-NMR (acetone-d_6) δ 7.50 (d, J = 7.5 Hz, 2H), 7.40 (d, J = 8.7 Hz, 2H), 7.32 (d, J = 7.5 Hz, 2H), 7.31 (m, 1H), 6.89 (d, J = 8.7 Hz, 2H), 3.78 (s, 3H); ^{13}C-NMR (acetone-d_6) δ 175.4, 160.0, 144.2, 136.0, 129.4, 128.5, 128.2, 113.9, 81.1, 55.4. **4,4′-Dimethoxybenzilic acid.** From 4,4′-dimethoxybenzil (Aldrich) in 60% yield: mp 159 °C (lit.[68] mp 155 °C); ^{1}H-NMR[68] (acetone-d_6) δ 7.39 (d, J = 8.7 Hz, 4H), 6.88 (d, J = 9.0 Hz, 4H), 3.81 (s, 6H); ^{13}C-NMR [68] (acetone-d_6) δ 159.5, 133.5, 132.4, 128.6, 113.5, 80.5, 55.3.

2,2′,5,5′-Tetramethoxybenzil. A solution of sodium cyanide (2.0 g) in 20 mL of water was added to a solution of 2,5-dimethoxybenzaldehyde (20 g, 0.12 mol) in 35 mL of absolute ethanol. The reaction mixture was stirred and refluxed for 0.5 h and then cooled to room temperature. An orange oily phase separated. The oil was washed with cold (0 °C) ethanol and dried *in vacuo*. This crude material (2,2′,5,5′-tetramethoxybenzoin) was dissolved in 70 mL of 80 vol % aqueous acetic acid. Ammonium nitrate (10 g, 0.125 mol) and cupric acetate (0.2 g) were added, and the reaction mixture was refluxed for 1.5 h. Upon cooling to room temperature, a yellow-orange solid precipitated from the solution. The crude tetramethoxybenzil was recrystallized from ethanol to yield 12 g (62%) of 2,2′,5,5′-tetramethoxybenzil as yellow rhombic crystals: mp 148−149 °C; ^{1}H-NMR (acetone-d_6) δ 7.48 (d, J = 3.0 Hz, 2H), 7.22 (dd, J = 8.7, 2.7 Hz, 2H), 7.10 (d, J = 8.7 Hz, 2H), 3.84 (s, 6H), 3.52 (s, 6H); ^{13}C-NMR (acetone-d_6) δ 192.4, 155.7, 155.0, 124.7, 123.1, 115.7, 112.8, 56.8, 56.0. Anal.[69] Calcd for $C_{18}H_{18}O_6$: C, 65.45; H, 5.49. Found: C, 65.29; H, 5.51. **2,2′,5,5′-Tetramethoxybenzilic Acid.** Prepared from 2,2′,5,5′-tetramethoxybenzil by the procedure of Ford-Moore[65] in 45% yield as the hemihydrate: mp 105−108 °C dec; ^{1}H-NMR (acetone-d_6) δ 7.02 (d, J = 3.0 Hz, 2H), 6.89 (dd, J = 8.7, 3.0 Hz, 2H), 6.82 (d, J = 3.0 Hz, 2H), 5.72 (br s, 3H), 3.73 (s, 6H), 3.66 (s, 6H); ^{13}C-NMR (acetone-d_6) δ 173.8, 154.5, 152.0, 131.4, 116.0, 114.2, 114.0, 79.6, 56.8, 55.8. Anal.[69] Calcd for $C_{18}H_{20}O_7 \cdot 0.5H_2O$: C, 60.50; H, 5.88. Found: C, 60.27; H, 5.86.

Methylviologen was prepared as the bis(trifluoromethanesulfonate) as follows: A solution of 4,4′-dipyridyl (3.12 g, 0.02 mol) in 50 mL of dichloromethane was stirred as methyl trifluoromethanesulfonate (6.56 g, 0.04 mol), dissolved in 50 mL of the same solvent, was added over a period of 15 min. During the addition, the solution became warm, and a white precipitate of methylviologen ditriflate formed. Diethyl ether (100 mL) was added to precipitate the remainder of the product. The white microcrystalline solid was recrystallized from a mixture of acetonitrile and ethyl acetate to afford thick

(61) (a) Asahi, T.; Mataga, N.; Takahashi, Y.; Miyashi, T. *Chem. Phys. Lett.* **1990**, *171*, 309. (b) Asahi, T.; Mataga, N. *J. Phys. Chem.* **1989**, *93*, 6575. (c) Asahi, T.; Mataga, N. *J. Phys. Chem.* **1991**, *95*, 1956. (d) Segawa, H.; Takehara, C.; Honda, K.; Shimidazu, T.; Asahi, T. Mataga, N. *J. Phys. Chem.* **1992**, *96*, 503. (e) Asahi, T.; Ohkohchi, M.; Mataga, N. *J. Phys. Chem.* **1993**, *97*, 13132. (f) Gould, I. R.; Noukakis, D.; Gomez-Jahn, L.; Goodman, J. L.; Farid, S. *J. Am. Chem. Soc.* **1993**, *115*, 4405.

(62) (a) Hubig, S. M. *J. Lumin.* **1991**, *47*, 137. (b) Hubig, S. M. *J. Phys. Chem.* **1992**, *96*, 2903. (c) Hubig, S. M.; Kochi, J. K. *J. Phys. Chem.* **1995**, *99*, 17578.

(63) (a) It is remarkable that the competing processes of back-electron transfer and carbon−carbon bond cleavage are completely independent and the rate of one process is not affected by the presence of the other. (b) A quantitative comparison is not possible at this juncture, however, since the thermodynamic oxidation potentials of the carboxylate donors are not directly available from electrochemical measurements. Owing to the rapid $C-CO_2$ bond cleavage in the acyloxy radical, accurate E_0 values for carboxylates cannot be obtained directly from electrochemical experiments.[64]

(64) Najdo, L.; Savéant, J.-M. *J. Electroanal. Chem.* **1973**, *48*, 113.

(65) Ford-Moore, A. H. *J. Chem. Soc.* **1947**, 952.

(66) Shacklett, C. D.; Smith, H. A. *J. Am. Chem. Soc.* **1953**, *75*, 2654.

(67) Ohwada, T.; Shudo, K. *J. Org. Chem.* **1989**, *54*, 5227.

(68) Ohwada, T.; Shudo, K. *J. Am Chem. Soc.* **1988**, *110*, 1862.

(69) Elemental analyses were performed by Atlantic Microlabs, Norcross, GA.

colorless plates of methylviologen ditriflate. Anal. Calcd for $C_{14}H_{14}F_6N_2O_6S_2$: C, 34.72; H, 2.91; N, 5.78. Found: C, 34.83; H, 2.87; N, 5.73.

Instrumentation. ^{1}H- and ^{13}C-NMR spectra were recorded on a General Electric QE-300 NMR spectrometer, and the chemical shifts are reported in ppm units downfield from tetramethylsilane. UV−vis absorption spectra were recorded on a Hewlett-Packard 8450A diode-array spectrometer. Gas chromatography was performed on a Hewlett-Packard 5890A gas chromatograph equipped with a flame-ionization detector and a HP 3392 integrator. GC−MS analyses were carried out on a Hewlett-Packard 5890A chromatograph interfaced to a HP 5970 mass spectrometer (EI, 70 eV). Melting points were measured on a Mel-Temp apparatus (Laboratory Devices) and are uncorrected. Time-resolved spectroscopic measurements on the picosecond and nanosecond/microsecond time scales were carried out with laser spectrometers described previously.[36]

Determination of Photochemical Quantum Yields. An aqueous solution of the sodium salt of the benzilate was prepared by addition of 0.5 mmol of the free acid and 0.090 g (0.55 mmol) of $NaHCO_3$ to 5.0 mL of distilled water. The solution was stirred until dissolution appeared to be complete and then filtered and transferred to a 1.0-cm Pyrex test tube. Methylviologen ditriflate (0.24 g, 0.5 mmol) was added, and the tube was closed by a rubber septum. The solution was then degassed by purging with argon for 30 min. The absorbance of these solutions at 366 nm was always greater than 2.0, to indicate that more than 99% of the incident light was absorbed.

The light source for the quantum yield measurements was a medium-pressure 500-W mercury lamp (Osram HBO) equipped with a circulating water filter to remove infrared radiation. The 366-nm line of the mercury emission spectrum was isolated by a combination of a $CoSO_4$ solution filter and colored-glass filters (Corning CS 0−52 and 7−37) as recommended by Murov *et al.*[71] The light flux was determined using Aberchrome-540 as the actinometer.[39] An actinometric measurement was carried out prior to each quantum yield determination, and the light flux remained essentially constant at $1.8 \pm 0.2 \times 10^{-7}$ einsteins min^{-1}. The solutions of $MV(OTf)_2$ and $Ar_2C(OH)CO_2Na$ were irradiated for 10−20 s until the faint blue color of $MV^{\bullet+}$ persisted unchanged upon stirring for 10 min. (This preirradiation removed residual oxygen from the reaction mixture.) The optical density of the solution at 604 nm was measured and taken as the initial absorbance (A_i). The solution was then irradiated for 1.0 min, and the final absorbance (A_f) was measured. The quantum yields were calculated as $\Phi_{SS} = [(A_f - A_i)/\epsilon_{MV}](V/F)$,[70] where V was the volume of the solution (5.0 mL), F the light flux in einsteins min^{-1}, and ϵ_{MV} the molar extinction coefficient of $MV^{\bullet+}$ in water (13 700 M^{-1} cm^{-1} at 605 nm[22]).

The quantum yields of the diaryl ketones were determined by quantitative gas chromatography using 4-chlorobenzophenone as the internal standard. Correction factors were calculated by coinjection of known amounts of authentic samples and the internal standard. Solutions were made up with the same volumes and concentrations as for the determination of the $MV^{\bullet+}$ quantum yields. For the quantum yields determined on the aerated samples (Φ_{aer} in Table 3), a slow stream of air (1−2 bubbles/s) was drawn through the solution during the irradiation. For the catalyzed reactions (Φ_{cat}), 11 mg of amorphous platinum dioxide (Adams catalyst, Strem) was added to the solution, which was then degassed. In both cases the blue color of $MV^{\bullet+}$ did not develop during the irradiation. After the photolysis, the aqueous solution was extracted three times with 2.0 mL portions of dichloromethane. The organic extracts were washed with saturated aqueous NaCl and dried over $MgSO_4$, and the internal standard was added. The yields of diaryl ketones were determined by GC analysis. Irradiation during a time period of 60−80 min was sufficient to yield 1.0−5.0 μmol of ketone.

Preparation of Samples for Time-Resolved Spectroscopy. Aqueous solutions 0.02−0.10 M in methylviologen ditriflate and 0.1−0.3 M in the sodium salt of the carboxylate acid were prepared for the experiments on the femtosecond/picosecond time scale. The absorbance at the irradiation wavelength was 1.0−1.6. Preliminary experiments indicated that the laser irradiation of degassed solutions generated large amounts of persistent $MV^{\bullet+}$, which interfered with the time-resolved spectroscopic measurements; accordingly, the solutions were prepared in the open atmosphere and not degassed. The sample cell was a 1.0 cm quartz flow cell, and the sample solution was circulated with a Labline 5514 peristaltic pump to minimize problems arising from secondary photolysis of the products. Connections were made with Teflon and Fluoran tubing. The UV−vis spectra of the circulating solution were acquired before and after the laser photolysis experiments to ensure that no significant thermal or photochemical changes had occurred.

The transient quantum yields of $MV^{\bullet+}$ upon excitation of the CT ion pairs were measured by the method of relative transient actinometry.[37] A solution of benzophenone (4.0×10^{-3} M) in deaerated benzene served as the actinometer, and the transient absorbance of the triplet of benzophenone, with $\lambda_{max} = 530$ nm and $\epsilon_{BP} = 7220$ M^{-1} cm^{-1} [37] was monitored. The absorbance was determined at three laser excitation energies. Solutions of $MV(OTf)_2$ (5−10 mM) and sodium carboxylate (0.02−0.05 M) were made up in the same cuvette as used for the actinometric measurements, and the concentrations were adjusted to match those of the actinometer solution. The solutions were then degassed by purging with argon. The transient absorbance of $MV^{\bullet+}$ was monitored at $\lambda_{max} = 605$ nm. This absorbance was observed to increase between 10 and 100 ns following the flash. The trace was linearly extrapolated to zero time to obtain A_{MV} for each laser excitation energy. Quantum yields were calculated using the following relation: $\Phi_{MV} = (A_{MV}/A_{BP})/(\epsilon_{MV}/\epsilon_{BP})$, where A_{BP} is the absorbance of benzophenone triplet and ϵ_{MV} and ϵ_{BP} are the extinction coefficient of $MV^{\bullet+}$ (13 700 M^{-1} cm^{-1} at 605 nm[22]) and benzophenone triplet (7220 M^{-1} cm^{-1} at 530 nm[37]), respectively. The values of Φ_{MV} so obtained were invariant (±10%) with laser energy over a range from 4 to 22 mJ per pulse.

The transient spectra of the ketyl radicals, diphenylhydroxymethyl and di-(*p*-tolyl)hydroxymethyl, were generated from the corresponding diaryl ketone using the nanosecond/microsecond laser spectrometer. The ketone (benzophenone or 4,4′-dimethylbenzophenone (ca. 4×10^{-3} M) was dissolved in a 1:1 (v:v) mixture of water and isopropyl alcohol. The concentration was adjusted so that the absorbance was 0.4 at 355 nm, and the solution was degassed by bubbling with argon for 30 min. Laser flash photolysis initially generated the ketones in their transient triplet state, which decayed within 10 μs to a residual absorbance of the ketyl radical. The band maximum and spectral width of the ketyl radical absorbance was essentially identical to that reported in aqueous media.[28,33]

Acknowledgment. We thank the National Science Foundation, the Robert A. Welch Foundation, and the Texas Advanced Research Program for financial support.

Supporting Information Available: The femtosecond laser spectrometer is described in detail, and the kinetics of the formation and decay of the radical pairs [$MV^{\bullet+}$, $Ar_2C(OH)$-$CO_2^{\bullet}$] are analyzed (5 pages). This material is contained in libraries on microfiche, immediately follows this article in the microfilm version of the journal, and can be ordered from the ACS; see any current masthead page for ordering information.

JO9617833

(70) See: de Mayo, P. In *Creation and Detection of the Excited State*; Ware, W. R., Ed.; Dekker: New York, 1976; Vol. 4, p 194.

(71) Murov, S. L.; Carmichael, I.; Hug, G. L. *Handbook of Photochemistry*; Dekker: New York, 1933; p 322.